accordion, a zebrafish behavioral mutant, has a muscle relaxation defect due to a mutation in the ATPase Ca^{2+} pump SERCA1

Hiromi Hirata[1], Louis Saint-Amant[1], Julie Waterbury[3], Wilson Cui[1], Weibin Zhou[1], Qin Li[1], Daniel Goldman[2], Michael Granato[3] and John Y. Kuwada[1,*]

[1]Department of Molecular, Cellular and Developmental Biology and [2]Mental Health Research Institute, University of Michigan, Ann Arbor, MI 48109-0720, USA
[3]Department of Cell and Developmental Biology, University of Pennsylvania School of Medicine, Philadelphia, PA 19104-6058, USA
*Author for correspondence (e-mail: kuwada@umich.edu)

Accepted 16 August 2004

Development 131, 5457-5468
Published by The Company of Biologists 2004
doi:10.1242/dev.01410

Summary

When wild-type zebrafish embryos are touched at 24 hours post-fertilization (hpf), they typically perform two rapid alternating coils of the tail. By contrast, *accordion* (*acc*) mutants fail to coil their tails normally but contract the bilateral trunk muscles simultaneously to shorten the trunk, resulting in a pronounced dorsal bend. Electrophysiological recordings from muscles showed that the output from the central nervous system is normal in mutants, suggesting a defect in muscles is responsible. In fact, relaxation in *acc* muscle is significantly slower than normal. In vivo imaging of muscle Ca^{2+} transients revealed that cytosolic Ca^{2+} decay was significantly slower in *acc* muscle. Thus, it appears that the mutant behavior is caused by a muscle relaxation defect due to the impairment of Ca^{2+} re-uptake. Indeed, *acc* mutants carry a mutation in *atp2a1* gene that encodes the sarco(endo)plasmic reticulum Ca^{2+}-ATPase 1 (SERCA1), a Ca^{2+} pump found in the muscle sarcoplasmic reticulum (SR) that is responsible for pumping Ca^{2+} from the cytosol back to the SR. As *SERCA1* mutations in humans lead to Brody disease, an exercise-induced muscle relaxation disorder, zebrafish *accordion* mutants could be a useful animal model for this condition.

Key words: Zebrafish, Accordion, Behavior, Muscle, Calcium, SERCA1, Brody disease

Introduction

Several factors have made the zebrafish an attractive vertebrate model for the study of motor development. First, forward genetics can be applied to zebrafish to identify genes that are essential for proper behaviors (Granato et al., 1996). Second, embryos are transparent, allowing the visualization of dynamic events, such as Ca^{2+} transients and axonal outgrowth in live fish (Fetcho and O'Malley, 1997; Lewis and Eisen, 2003). Third, electrophysiological techniques can be used to analyze the physiology of embryonic neurons and muscles to dissect embryonic behaviors (Drapeau et al., 2002). Fourth, zebrafish embryos exhibit readily assayable and well-characterized behaviors (Eaton and Farley, 1973; Saint-Amant and Drapeau, 1998).

Zebrafish embryos display three stereotyped behaviors by 36 hours post-fertilization (hpf) (Saint-Amant and Drapeau, 1998). The earliest behavior consists of repetitive spontaneous alternating coiling of the tail, much like a metronome. This simple slow coiling behavior is independent of stimulation and starts at 17 hpf, reaches a peak frequency of 1 Hz at 19 hpf, and declines to less than 0.1 Hz by 26 hpf. After 21 hpf, embryos start to respond to mechanosensory stimulation with coils that are stronger than spontaneous coils. Typically embryos respond with two alternating coils. By 26 hpf mechanosensory stimulation initiates swimming episodes. The frequency of muscle contractions during swimming increases from 7 Hz at 26 hpf to 30 Hz at 36 hpf, the latter being similar to the frequency of swimming of adult zebrafish (Buss and Drapeau, 2001).

The production of any touch response can be divided into several steps from sensory perception to muscle activation (reviewed by Roberts, 2000; Berchtold et al., 2000). In zebrafish, two types of mechanosensory neurons sense touch stimuli. Head and yolk stimulation acts through trigeminal neurons, whereas tail stimulation activates Rohon-Beard neurons (Drapeau et al., 2002). Once triggered by sensory input, interneuronal networks located in the hindbrain and spinal cord produce the appropriate motor rhythm (Fetcho, 1992). Motoneurons are activated by these central networks, release acetylcholine at neuromuscular junctions (NMJs) and depolarize the muscle membrane (Buss and Drapeau, 2002; Li et al., 2003). In muscle, depolarization is sensed by voltage-dependent L-type Ca^{2+} channels, such as dihydropyridine receptors, and activates ryanodine receptors in the sarcoplasmic reticulum (SR) membrane to release Ca^{2+} from the SR to the cytosol (Fill and Copello, 2002). Increased cytosolic Ca^{2+} activates troponin C that initiates actin/myosin sliding, thus contracting the muscles (Gordon et al., 2000). Cytosolic Ca^{2+} levels are rapidly decreased by sarco(endo)plasmic reticulum Ca^{2+}-ATPase 1 (SERCA1), a Ca^{2+} pump expressed in skeletal muscle, which enables relaxation (McLennan et al., 1997).

Any defect in the above pathway induces motor disorder in human. For example, impairment of Ca^{2+} regulation by *SERCA1* mutation in human causes Brody disease, a rare inherited disorder of skeletal muscle function (Odermatt et al., 1996). The clinical signs and symptoms in individuals involve exercise-induced impairment of muscle relaxation, stiffening and cramps (Brody, 1969; MacLennan, 2000). In fact, in vitro study with cultured muscle cells from individuals with this disease revealed slow Ca^{2+} reuptake and reduced Ca^{2+}-ATPase activity that can explain the relaxation defect (Benders, 1994).

The large-scale Tübingen mutagenesis screen isolated 63 behavioral mutants that displayed abnormal touch responses between 48 and 60 hpf (Granato et al., 1996). Some of the locomotion mutants, raised in this screen as well as the others, were further characterized. Reduced touch sensitivity mutants such as *macho*, *alligator* and *steifftier* had defects of Na^{+} channel function in mechanosensory Rohon-Beard neurons (Ribera and Nüsslein-Volhard, 1998). *shocked* mutants, which showed abnormal swimming, were defective in motor processing in the central nervous system (CNS) (Cui et al., 2004). Reduced or abnormal motility mutants *diwanka*, *unplugged* and *space cadet* had defects in axon projections (Zeller and Granato, 1999; Zeller et al., 2002; Zhang and Granato, 2000; Zhang et al., 2001; Lorent et al., 2001). Immotile or reduced motility mutants, such as *nic/twister*, *sofa potato*, *ache/zieharmonika* and *twitch once*, were defective at the NMJ (Westerfield et al., 1990; Lefebvre et al., 2004; Ono et al., 2001; Behra et al., 2002; Downes and Granato, 2004; Ono et al., 2002). Another immotile mutant, *relaxed*, had a coupling defect between muscle excitation and contraction (Ono et al., 2001). Mutants carrying reduced striations in somatic muscles, such as *fibrils unbundeled* and *sapje*, were shown to have abnormal myofiber organization (Felsenfeld et al., 1990; Bassett et al., 2003). The genes mutated in the mutants *nic/twister*, *sofa potato*, *ache/zieharmonika*, *twitch once* and *sapje* were, respectively, identified as the α-subunit of the *nicotinic acetylcholine receptor*, the δ-subunit of the *nicotinic acetylcholine receptor*, *acetylcholinesterase*, *rapsyn* and the *Duchenne muscular dystrophy* gene (Sepich et al., 1998; Lefebvre et al., 2004; Ono et al., 2004; Behra et al., 2002; Downes and Granato, 2004; Ono et al., 2002; Bassett et al., 2003).

Another zebrafish mutation, *accordion* (*acc*), exhibited apparent simultaneous contractions of trunk muscles on both sides of the embryo resulting in the shortening of the trunk in response to touch and was named in analogy to the action of the musical instrument (Granato et al., 1996). As application of a glycine receptor blocker, strychnine, to wild-type embryos phenocopied the abnormal behavior, it was proposed that the *acc* phenotype was due to defects in glycine-mediated transmission within the CNS (Granato et al., 1996). Agreeing with this anticipation, inhibitory glycine-mediated transmission is essential to prevent simultaneous, bilateral muscle contractions in a variety of vertebrates (Fetcho, 1990; Grillner, 2003; Kudo et al., 2004; Roberts, 2000). However, the *acc* phenotype can, in principle, be generated in a variety of other ways. As muscle defects can result in abnormal behavior (Bassett et al., 2003; Granato et al., 1996; Lefebvre et al, 2004; Ono et al., 2002), one of these ways could be via a muscle defect that increases the duration of muscle contractions without any defects in the alternation or timing of output from motoneurons in the two sides of the spinal cord. Such a defect would result in overlap of contractions on the two sides and shortening of the trunk.

In this paper, we have used electrophysiology to show that the output of the CNS and the function of the NMJ are normal in *acc*. However, after active contraction, *acc* truck muscles stiffened for a while and relaxation was five times slower than that in wild-type siblings. There was a correlated slowing of the decay of cytosolic Ca^{2+} transients in mutant muscles. These results suggested impaired Ca^{2+} re-uptake into the SR from the cytosol in mutant muscles. Indeed, application of thapsigargin, an inhibitor of SERCA, to wild-type embryos phenocopied *acc* defects. We identified mutations in the *atp2a1* gene, which encodes SERCA1, of *acc* mutants. The molecular identification of the *atp2a1/acc* gene was confirmed by rescue of the mutant phenotype by injection of wild-type *atp2a1* mRNA into mutant embryos and by phenocopy of the mutation by injection of antisense *atp2a1* morpholino oligonucleotides (MO) into wild-type embryos. Mutations in *ATP2A1* in humans are known to cause Brody disease, an exercise-induced muscle relaxation disorder (Brody, 1969; Odermatt et al., 1996), making the *acc* mutant an attractive animal model for Brody disease.

Materials and methods

Animals

Zebrafish were bred and raised according to established procedures (Westerfield, 1995; Nüsslein-Volhard and Dahm, 2002), which meet the guidelines set forth by the University of Michigan animal care and use protocols. *acc*^{tq206} was generated from the large-scale Tübingen screen (Granato et al, 1996). *acc*^{mi25i} and *acc*^{mi289a} were isolated in our behavioral screen. Zebrafish were mutagenized by following published procedures (Mullins et al., 1994).

Video recording of zebrafish behavior and muscle contraction

Embryonic behaviors were observed and video recorded using a dissection microscope. Mechanosensory stimuli were delivered to the yolk with forceps. For closer examinations of muscle contractions, 24 hpf embryos were anaesthetized (0.02% tricaine) and pinned with tungsten wires (25 μm diameter) through the notochord onto a silicon elastomer (Sylgard)-lined dish in Evans solution (134 mM NaCl, 2.9 mM KCl, 2.1 mM $CaCl_2$, 1.2 mM $MgCl_2$, 10 mM glucose, and 10 mM HEPES at 290 mOsm and pH 7.8). Tricaine was removed by replacing the tricaine/Evans solution with Evans with no tricaine. Mechanosensory stimuli were delivered to the yolk by ejecting bath solution (20 psi, 20 mseconds pulse) from a pipette with a 15-30 μm tip using a Picospritzer II (General Valve Corporation). Several somites were observed in high resolution with Hoffman modulation optics (40× water immersion objective). Videos were captured with a CCD camera (WVBP330, Panasonic) and a frame grabber (LG-3, Scion Corporation) and analyzed with Scion Image on a G4 Macintosh. The contraction and relaxation durations were measured by counting frames from the videos (1 frame=33 mseconds).

Kinetic analysis of muscle contraction

Embryos at 24 hpf were anaesthetized and pinned to a Sylgard dish in Evans solution. Tungsten wires were put through the forebrain, because the intact forebrain and midbrain are not necessary for the touch response and spontaneous contractions at 24 hpf (Saint-Amant and Drapeau, 1998). Tricaine/Evans was replaced with Evans containing no tricaine and mechanosensory stimuli delivered to the tail for the touch response. Videos were captured and analyzed with

Scion Image. The durations for active contraction, constant contraction and relaxation were measured by counting frames (1 frame=33 mseconds).

Muscle recording

The dissection protocols for in vivo patch recordings have been described previously (Buss and Drapeau, 2000). Briefly, 48 hpf zebrafish embryos were anaesthetized in tricaine and pinned on a Sylgard dish. The skin was peeled off to allow access to the underlying muscle cells. For electrophysiological recordings, embryos were partially curarized in an Evans solution containing 6 μM d-tubocurarine but not tricaine. Patch electrodes were pulled from borosilicate silicate glass to yield electrodes with resistances of 6-10 MΩ. The patch electrode was visually guided to patch muscle cells using Hoffman modulation optics (40× water immersion objective). The electrode solution was consisted of 105 mM potassium gluconate, 16 mM KCl, 2 mM $MgCl_2$, 10 mM HEPES, 10 mM EGTA and 4 mM Na_3ATP at 273 mOsm and pH 7.2. Recordings were performed with an Axopatch 200 amplifier (Axon Instruments), low-pass filtered at 5 kHz, and sampled at 10 kHz. Data was collected with Clampex 8.2 software (Axon Instruments) and analyzed with Clampfit 9.0 software (Axon Instruments). Mechanosensory stimulation to induce fictive swimming was delivered by ejecting bath solution (20-50 psi, 10-30 mseconds pulse) from a pipette with a 15-30 μm tip using a Picospritzer II to the tail of the pinned embryo.

Muscle contractions by current injection

As described previously, it is possible to inject current through a patch to evoke muscle contractions in live zebrafish and still maintain the whole cell configuration (Buss and Drapeau, 2000). Embryos were completely curarized with an Evans solution containing 15 μM d-tubocurarine. The current intensity and the current pulse duration were set to 2-7 nA and 15-20 mseconds, respectively, which were sufficient to evoke a contraction. This condition mimics the cycle duration of motoneurons output that must be occurring for the embryo to swim at the observed tail beat frequencies of 30 Hz (Buss and Drapeau, 2001). The contractions of the muscle were observed on a video monitor and captured with a CCD camera to analyze with a computer.

Pharmacological treatment

Thapsigargin (10 mM stock in DMSO, Sigma) was diluted to 1 μM in Evans solution and applied to embryos 1 hour before assay.

Ca^{2+} imaging

We injected Calcium Green-1 dextran (10,000 M_r, Molecular Probes) into 1- to 4-cell stage embryos from *acc* carrier in-crosses. At later stages, random subsets of cells including muscles were seen to contain Calcium Green-1 dextran. The genotype of the injected embryos (24 and 48 hpf) was determined by responses to touch and the embryos were anaesthetized with 0.02% tricaine and pinned to a Sylgard dish. The tricaine was washed out and embryos were bathed in Evans solution containing a muscle myosin inhibitor, N-benzyl-p-toluene sulphonamide at 5 mM (Sigma), which does not affect to the Ca^{2+} regulation (Cheung et al., 2001). This drug suppressed the muscle contractions and enabled us to observe the Ca^{2+} transients with a confocal microscope (LSM510, Carl Zeiss). As plane-scanning requires too much time to adequately measure Ca^{2+} transients, we performed line-scanning at 132 Hz (7.6 mseconds/scan) of a fluorescent muscle cell. The time course of the average strength of fluorescence in the line at each scan was calculated with the maximum fluorescence of each record equalized. The observed changes in fluorescence indicate Ca^{2+} transients during spontaneous coiling at 24 hpf. *N*-methyl-D-aspartate (NMDA, 50 μM) was bath applied to 48 hpf embryos to activate swimming (Cui et al., 2004), as spontaneous movement was hardly observed at 48 hpf (Saint-Amant et al., 1998).

Meiotic and physical mapping

acc carrier fish (Tübingen strain) were crossed with wild-type WIK fish to generate mapping carriers that were crossed to identify mutants for meiotic mapping to microsatellites and genes using PCR as described previously (Nüsslein-Volhard and Dahm, 2002; Gates et al., 1999; Shimoda et al., 1999). For mapping *acc* against *netrin 1*, a polymorphism of the *Dra*I restriction site in a 136 bp PCR product (forward primer, 5′-GCATATGAAATATGATAGAGGAAGATT-3′; reverse primer, 5′-TGAAACAAGTCTGCTTGAACCAG-3′) found in the map crosses was used. The LN54 radiation hybrid panel was used for the physical mapping (Hukriede et al., 1999).

Cloning, knockdown, mRNA rescue, and mutagenesis of *ATP2A1*

The following primers were used for cloning of *ATP2A1* cDNA: forward primer, 5′-GGGGCCATCTGTTTTGTCCCTATCCTTCAC-3′; reverse primer, 5′-GGGTGATTTTTCACTGGTTCCCGGTTGG-3′. To knock down the protein synthesis (Summerton and Weller, 1997), SERCA1 antisense MO (5′-CGTTCTC**CAT**CCTGTCTGC-TCAAAG-3′) was designed against 16 mer of 5′-UTR sequence and adjacent 9 mer coding region on mRNA. The **CAT** sequence in bold corresponds to the start ATG. Standard control MO (randomized sequence available from Gene Tools) was used for control MO. Capped *atp2a1* mRNA synthesis was performed with mMESSAGE mMACHINE T7 Ultra (Ambion). The 5′-UTR sequence of the synthesized mRNA was amended (5′-CCTCGAGCCGCCACC**AT-G**GAGAACGCA-3′) in order to avoid knockdown by the antisense MO. The **ATG** sequence in bold is the start ATG. Injections (0.25 mM for MO and 1 μg/μl for mRNA) were performed as described previously (Xiao et al., 2003; Nüsslein-Volhard and Dahm, 2002). The Pro789Leu mutation (CCA to CTG), previously identified as a mutation underlying Brody disease (Odermatt et al., 2000), was introduced into the zebrafish *atp2a1* construct by the Quick Change method (Stratagene) with the following primers: forward primer, 5′-CCTGAGGCTCTGATC**CTG**GTTCAGCTGCTGTGG-3′; reverse primer, 5′-CCACAGCAGCTGAAC**CAG**GATCAGAGCCTCAGG-3′. The **CTG** and **CAG** sequence in bold indicates the sense and antisense codon, respectively, of the introduced Leu residue.

Immunostaining and in situ hybridization

Immunostaining was carried out as described previously (Devoto et al., 1996). Briefly, embryos at 24 hpf were anesthetized (0.02% tricaine), fixed in 4% paraformaldehyde and then washed several times in 0.1 M phosphate-buffered saline (PBS), pH 7.4. Embryos were blocked in PBS containing 2% BSA and 2% sheep serum, incubated in F59 antibody (anti-slow twitch myosin, 1:20, Developmental Studies Hybridoma Bank) diluted in PBS, and washed in PBS. Alexa 488-conjugated anti-mouse IgG was used as a secondary antibody (1/1000, Molecular Probes). In situ hybridization was performed as described previously (Li et al., 2004).

Mixture of two *atp2a1* probes covering nucleotides 1~997 (N terminus~M4 domain in SERCA1 protein) and 2598~3220 (M7~C terminus) were used for in situ hybridization. For sectioning after color development, embryos were equilibrated in 15% sucrose/7.5% gelatin in PBS at 37°C and then embedded in it at –80°C. Sections (20 μm) were cut with a cryostat (CM3050S, Leica).

Results

Relaxation by muscles is significantly slower in *acc* mutants

As part of an ongoing ENU mutagenesis screen, we isolated two new alleles (mi25i and mi289a) of *acc* that were autosomal recessive and lead to death by 10 days (not shown). We performed phenotypic analysis on the original *acc* allele (tq206) from Tübingen (Granato et al., 1996), because it

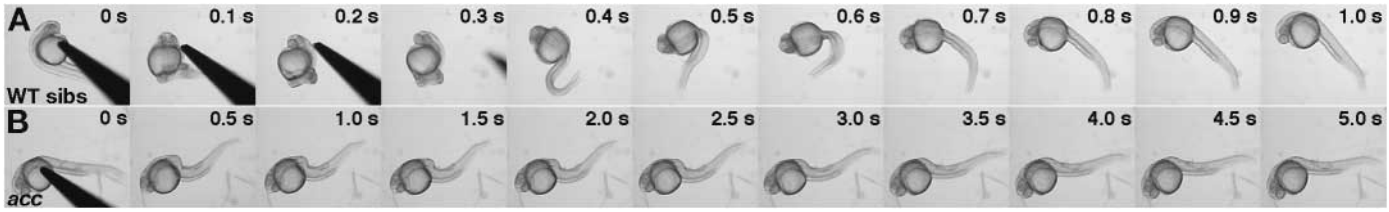

Fig. 1. *acc* embryos exhibit an aberrant response to touch. Embryos (24 hpf) were stimulated by touching them with forceps. (A) Touch induced a wild-type embryo to coil twice within 1 second. Relaxation of the trunk after the second coil took less than 0.5 seconds. (B) Touch induced an *acc* embryo to contract both sides in an apparent simultaneous fashion to cause the trunk to bend dorsally followed by a slow relaxation (>4 seconds).

displayed the strongest phenotype as described below. When wild-type embryos were touched with forceps at 24 hpf, they reacted with two or three fast, alternating coils of the tail that immediately followed each other (Fig. 1A, see Movie 1 in the supplementary material). By contrast, *acc* embryos appeared to simultaneously contract the trunk axial muscles on both sides and this resulted in a dorsal flexure of the trunk (Fig. 1B, see Movie 2 in the supplementary material). The mutants stayed in a contracted state long after wild-type embryos have relaxed. To examine a muscle movement at higher resolution, we observed a contraction of several somites in embryos loosely pinned on a Sylgard dish and stimulated to evoke a contraction. Although wild-type embryos displayed quick muscle contractions (0.61±0.03 seconds, n=5, see Movie 3 in the supplementary material), *acc* embryos showed significantly slower contractions (4.80±0.28 seconds, n=5, see Movie 4 in the supplementary material). At 48 hpf, wild-type siblings swim away when touched, whereas *acc* mutants failed to swim (data not shown). The *acc* larvae died at 7-10 days post-fertilization, possibly from the inability to swim and feed effectively.

To compare the three alleles of *acc* mutants with wild type, we measured the time course of active contraction when muscles are shortening, constant contraction when muscles are contracted but not changing in length, and relaxation when muscles are lengthening in responses to mechanosensory stimulation at 24 hpf (Table 1). The duration of the active contraction phase was not significantly different between wild-type siblings and *acc* mutants, whereas the relaxation phase took five times longer in all the alleles of *acc* compared with wild-type siblings. Furthermore, the constant contraction period was significantly longer (1.7~2 seconds) in *acc* embryos, whereas this stiffness was not observed (less than 0.1 second) in wild-type siblings. Among three alleles of *acc* mutants, tq206 showed the strongest phenotype in terms of the relaxation kinetics.

Mutant embryos spontaneously coiled at 24 hpf with normal frequency (0.27±0.02 Hz for wild type, n=10; 0.25±0.02 Hz for *acc*, n=10), but the kinetics of coiling was aberrant. The duration of the active contraction phase was not significantly different between wild-type siblings and *acc*, but the relaxation phase and constant contraction period were significantly longer in *acc* than in wild-type siblings (Table 1). Thus, the mutation appears not to perturb the ability to spontaneous coil, but rather results in prolonged coils. These observations suggest that rhythmic output from the CNS underlying spontaneous coiling is not perturbed in *acc* embryos but muscle relaxation is aberrant in mutants.

A significant increase in the duration of relaxation in *acc* embryos should decrease the stimulation frequency at which tetanus occurs. To test this, we stimulated muscles by injecting current with a patch electrode and video recorded the resultant contractions in mutant and wild-type siblings at 48 hpf. Wild-type muscles followed trains of depolarizations at frequencies from 1 to 35 Hz (n=5), whereas *acc* muscles followed at lower frequencies but failed to follow trains of depolarizations at 15±1.4 Hz (n=5), showing that *acc* muscles do reach tetanus at lower stimulation frequencies compared with wild-type

Table 1. The time course of constant contraction and relaxation phases but not active contraction phase is aberrant in *acc* mutants

	Touch responses at 24 hpf		
	Active contraction	Constant contraction	Relaxation
Wild-type sibs (n=7)	0.43±0.02 seconds	0.07±0.01 seconds	0.48±0.04 seconds
acc^{tq206} (n=7)	0.44±0.04 seconds	2.03±0.10 seconds*	2.68±0.13 seconds*
acc^{mi25i} (n=7)	0.45±0.03 seconds	1.81±0.07 seconds*	2.51±0.09 seconds*
acc^{mi289a} (n=7)	0.44±0.02 seconds	1.70±0.08 seconds*	2.42±0.09 seconds*
	Spontaneous coils at 24 hpf		
	Active contraction	Constant contraction	Relaxation
Wild-type sibs (n=10)	0.47±0.03 seconds	0.12±0.01 seconds	0.52±0.05 seconds
acc^{tq206} (n=10)	0.48±0.04 seconds	2.05±0.09 seconds*	2.81±0.19 seconds*
acc^{mi25i} (n=10)	0.45±0.03 seconds	1.86±0.08 seconds*	2.72±0.16 seconds*
acc^{mi289a} (n=10)	0.44±0.02 seconds	1.85±0.07 seconds*	2.67±0.14 seconds*

Time given indicates mean±s.e.m.
*P<0.01 (Student's t-test).

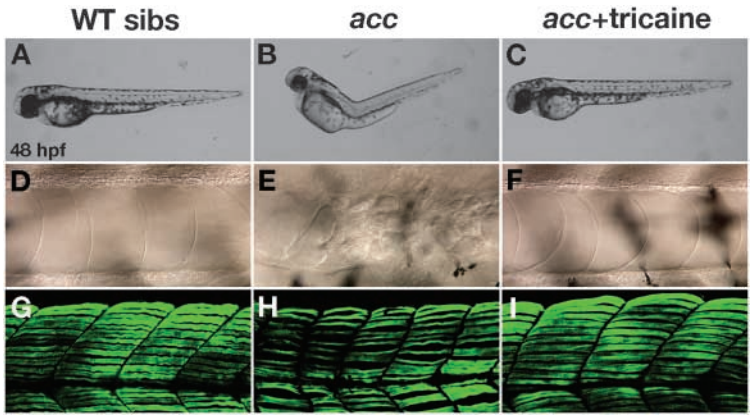

Fig. 2. Morphological defects observed at 48 hpf in *acc* embryos are secondary to the abnormal behavior. Tricaine is applied to *acc* embryos from 24 to 48 hpf to immobilize the embryos. Wild-type sibling and a tricaine-treated *acc* embryo (C) display a straight trunk while an *acc* mutant (B) displays a bent trunk. DIC images show that the notochord in a wild-type sibling (D) and tricaine-treated *acc* embryo (F) are undamaged, while the notochord of an *acc* mutant is breaking apart (E). The normal pattern of slow twitch muscle fibers labeled with MAb F59 is seen in wild-type sibling (G) and tricaine-treated *acc* mutant (I), but the slow twitch fibers are disarrayed in *acc* mutants (H).

muscles. This result, along with the relaxation data, strongly suggests that one site of defect in the mutants is muscle and that the overlap in muscle contractions on the two sides due to the slow relaxation causes the shortening of the trunk seen in *acc* embryos during an escape response following a mechanosensory stimulus.

In addition to behavioral defects, *acc* embryos exhibited morphological defects (Granato et al., 1996). After 48 hpf, the trunks of *acc* embryos were frequently bent (Fig. 2A,B) and this phenotype worsened with age (not shown). Disruption of the notochord was also observed after 36 hpf (Fig. 2D,E). Labeling of slow twitch muscle fibers in *acc* with mAb F59 (Devoto et al, 1996) showed that they were disturbed (Fig. 2G,H), but no increased cell death assayed with TUNEL and Acridine Orange labeling was observed (data not shown). These morphological defects were probably secondary ones resulting from the mechanical stress caused by the aberrant contractions. Supporting this idea, prolonged treatment with tricaine, a weak Na^+ channel inhibitor that prevented motor behavior, abolished the morphological defects in *acc* mutants (Fig. 2C,F,I). Treatment with N-benzyl-p-toluene sulphonamide, a specific inhibitor of muscle myosin, also prevented the morphological defects (data not shown).

Output of the CNS and the NMJ appears normal in *acc* embryos

The production of any motor behavior can be divided into several steps, such as sensory perception, production of rhythmic activity in the CNS, synaptic transmission at the NMJ, Ca^{2+} regulation in muscle cell, and contraction of muscle (reviewed by Roberts, 2000; Fetcho, 1992; Berchtold et al., 2000). The fact that muscle relaxation is much slower in *acc* embryos suggests that one site of defect is muscle. However, it remains possible that processes preceding muscle relaxation may also be defective. As application of strychnine, a blocker of glycine-mediated inhibitory synaptic transmission, phenocopies *acc*-like bilateral contractions following mechanosensory stimulation (Granato et al, 1996), one possibility is that inhibitory interactions within the CNS are also defective in *acc*. To examine this, we demonstrated both CNS morphology and physiology of mutants at the NMJ.

The overall morphology of the CNS, including the hindbrain and spinal cord, which are necessary and sufficient for the early behaviors in zebrafish, was not obviously perturbed in *acc* embryos (data not shown). The pattern of the hindbrain reticulospinal interneurons, spinal Rohon-Beard sensory neurons, and spinal motoneurons and their axons labeled with anti-acetylated α-tubulin (which labels all axons) (Chitnis and Kuwada, 1990; Bernhardt et al., 1990) and anti-Islet (which labels Rohon-Beard and motoneurons nuclei) (Korzh et al., 1993) were normal (data not shown). Furthermore, the pattern of α-bungarotoxin-labeled acetylcholine receptor on muscles (Ono et al., 2001) was normal (data not shown).

The physiological output from the CNS at the NMJ was

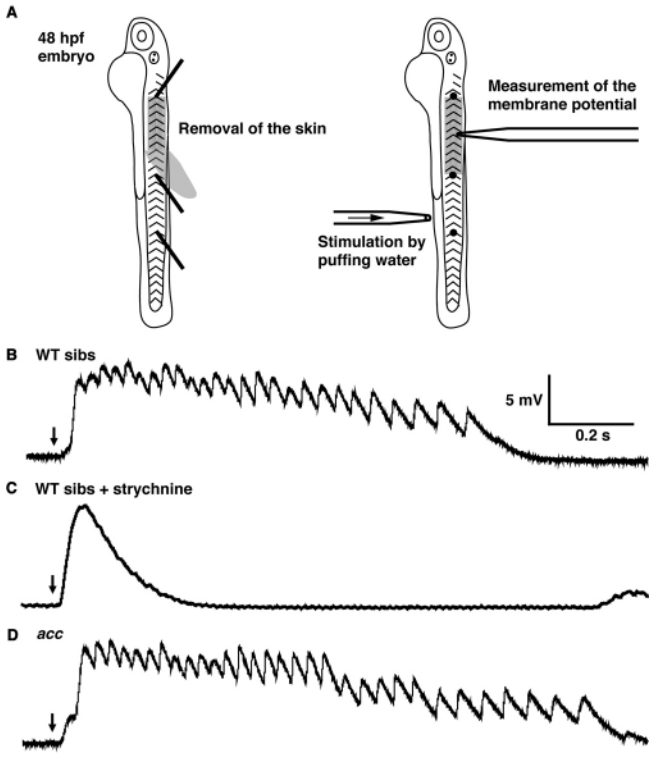

Fig. 3. The CNS and the NMJ are normal in *acc*. (A) Schematic summary of the experimental procedure. Embryos (48 hpf) are pinned on a dish through the notochord. The skin is peeled off to allow access to the muscle cells. Muscle voltage responses are evoked by mechanosensory stimulation delivered by a puff of water and are measured with a patch electrode. Wild-type siblings (B) and *acc* (D) display similar rhythmic depolarizations (fictive swimming), whereas strychnine-treated wild-type siblings (C) respond with a non-rhythmic, shorter depolarization.

assayed by in vivo patch recordings from trunk axial muscle of 48 hpf embryos (Fig. 3A). Muscle voltage recordings from wild-type sibling embryos showed sustained episodes of rhythmic depolarizations following mechanosensory stimulation (Fig. 3B). This rhythmic activity had a frequency (25 to 30 Hz) that was comparable with the swimming frequency observed during free swimming and presumably underlies swimming contractions (Buss and Drapeau, 2001). The average duration of the muscle response in wild-type siblings was 1.28±0.22 seconds (n=10) and maximum amplitude was –54.1±1.0 mV. When strychnine (2 μM) was added to the bath solution, the pattern of activity in the muscle following mechanosensory stimulation dramatically changed so that the responses were shorter (0.29±0.03 seconds, n=10, Student's t-test, P<0.01) and lost their fast rhythmic activity, although the maximum amplitude (–54.9±1.0 mV) was comparable with wild-type siblings (Fig. 3C). Muscle recordings from *acc* embryos following mechanosensory stimulation showed a rhythmic voltage response in which the duration (1.38±0.22 seconds, n=10), maximum amplitude (–54.8±0.8 mV) and rhythmicity (25-30 Hz) were indistinguishable from that seen in wild-type siblings (Fig. 3D). Thus, the muscle recordings in *acc* embryos are similar to that in wild-type siblings and do not resemble the output of the CNS when glycine-mediated inhibitory transmission is blocked by strychnine. These results are consistent with the hypothesis that the output from the CNS and the response of the NMJ following mechanosensory stimulation is unperturbed in mutants and that the defect resides in muscle.

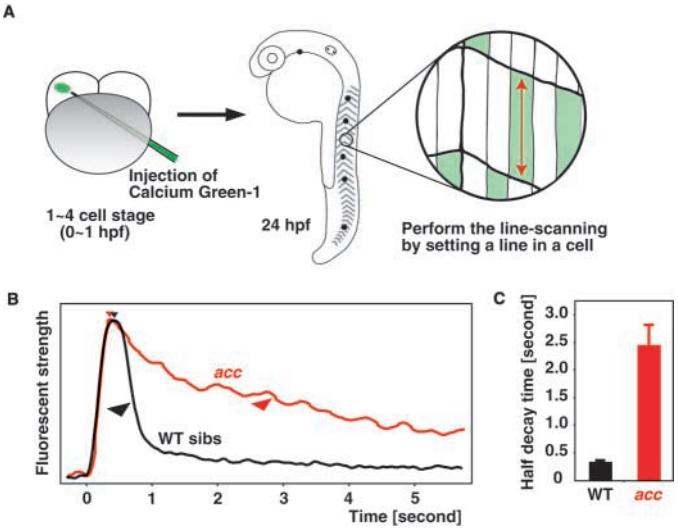

Fig. 4. Decay in Ca^{2+} transient is slower in *acc* muscles during relaxation. (A) Schematic summary of the experimental procedures. Calcium Green 1 dextran is injected into ~1- to 4-cell stage embryos. At 24 hpf embryos are pinned on a dish and mosaically fluorescent muscle cells are observed by line-scanning with a confocal microscope during spontaneous coiling. (B) There is no difference in the timing of the increase in fluorescence during Ca^{2+} transients between wild-type siblings (black) and *acc* (red) embryos, but the decay of fluorescence is much slower in mutant embryos. Small and large arrowheads indicate the peak and half decay of fluorescence, respectively. (C) Quantification of the difference in time to half decay from peak fluorescence. Ca^{2+} decay is slower in *acc* muscles than in wild-type siblings.

Decay in cytosolic Ca^{2+} transient is slower in *acc* muscles during relaxation

Depolarization of the muscle membrane leads to a transient increase of cytosolic Ca^{2+} that cause contraction and relaxation of muscle by actin/myosin sliding (Berchtold et al., 2000). As there is a muscle relaxation defect in *acc* mutants, we examined whether the regulation of intracellular Ca^{2+} is defective in mutant muscles. To visualize Ca^{2+} levels in live zebrafish, embryos were injected with Calcium Green-1 dextran, pinned on a Sylgard dish and imaged during a spontaneous coiling at 24 hpf by using a confocal microscope (Fig. 4A). As plane-scanning takes too long (>0.3 seconds/scan) to capture the Ca^{2+} transients, we performed line-scanning of muscles at 132 Hz (7.6 mseconds/scan, see Materials and methods). The time course of Ca^{2+} increase in *acc* muscle was indistinguishable from that of wild-type muscles, but the decay was significantly slower in the mutants (Fig. 4B,C). The time to decrease to half amplitude of Ca^{2+} (half decay) was seven times longer in *acc* (2.47±0.37 seconds, n=28) than in wild type (0.35±0.03 seconds, n=28; Student's t-test, P<0.01). We also examined Ca^{2+} transients in muscles of 48 hpf embryos during swimming (data not shown). Similar to Ca^{2+} transients during spontaneous coiling, the half decay of Ca^{2+} during swimming was significantly slower in *acc* muscles compared with that of wild-type siblings (*acc*, 0.94±0.06 seconds, n=10; wild-type siblings, 0.08±0.01 seconds, n=10; Student's t-test, P<0.01). Thus, the clearance of Ca^{2+} from the cytosol is much slower in *acc* muscles compared with that in wild-type muscles, as predicted by the differences in relaxation kinetics between mutant and wild-type muscles. As Ca^{2+} removal from the cytosol is accomplished mainly by SERCA1, a Ca^{2+} pump found in the SR that enables relaxation (MacLennan et al., 1997), our results are consistent with a defect in SERCA1 in *acc* embryos.

If SERCA1 is mutated in *acc* embryos, thapsigargin, a specific blocker of SERCA (Treiman et al., 1998), should phenocopy the mutation. Treatment of 24 hpf wild-type embryos with 1 μM thapsigargin resulted in touch-induced muscle contractions on the two sides of the trunk to overlap just as in *acc* embryos (data not shown). In addition, stimulation of muscle contraction by direct current injection revealed that thapsigargin-treated wild-type muscle cells failed to follow the stimulation at frequencies above 15 Hz (n=2), much like *acc* mutants. The Ca^{2+} imaging results and phenocopy by thapsigargin are consistent with the notion that a defect in SERCA1 causes the *acc* phenotype.

acc encodes for SERCA1

To identify the gene responsible for the *acc* mutation, we meiotically mapped the mutation to two flanking markers, z4161 (6.8 cM, 246 recombinants in 3616 meioses) and *netrin 1* (0.2 cM, 5 recombinants in 2448 meioses), in linkage group 3. As the *acc* phenotype suggested a defect in SERCA1, we physically mapped *atp2a1* gene that encodes SERCA1 using the LN54 radiation hybrid panel and found it to be close (4.3 cR) to *netrin 1* in linkage group 3 (Fig. 5A).

To test whether *atp2a1* contains mutations, we cloned and sequenced SERCA1 cDNA, which encodes 997 amino acid residues (GenBank Accession Number AB178533). SERCA1 contained 10 transmembrane domains (M1-M10) as well as a nucleotide-binding and a phosphorylation domain (Fig. 5B). A

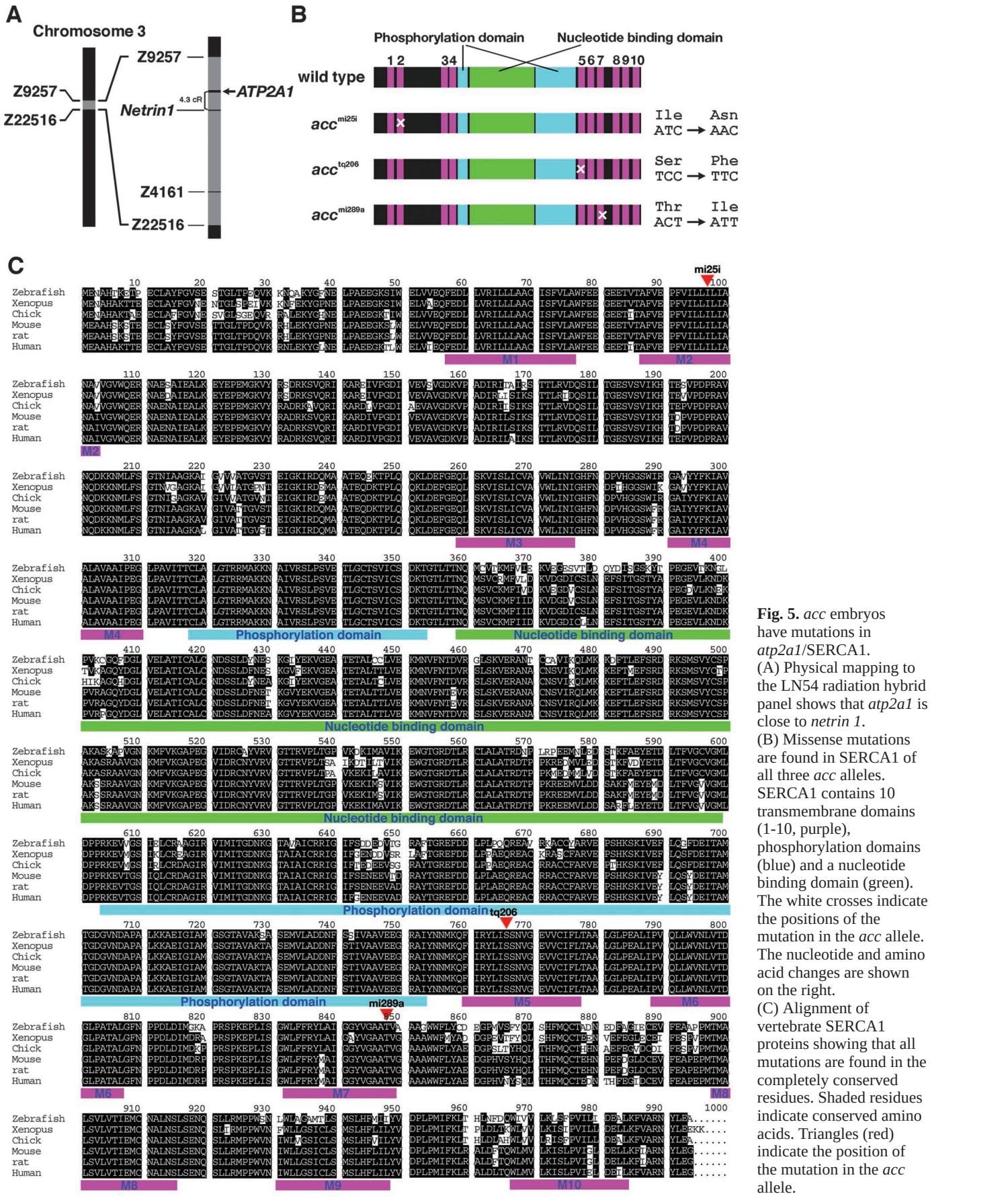

Fig. 5. *acc* embryos have mutations in *atp2a1*/SERCA1. (A) Physical mapping to the LN54 radiation hybrid panel shows that *atp2a1* is close to *netrin 1*. (B) Missense mutations are found in SERCA1 of all three *acc* alleles. SERCA1 contains 10 transmembrane domains (1-10, purple), phosphorylation domains (blue) and a nucleotide binding domain (green). The white crosses indicate the positions of the mutation in the *acc* allele. The nucleotide and amino acid changes are shown on the right. (C) Alignment of vertebrate SERCA1 proteins showing that all mutations are found in the completely conserved residues. Shaded residues indicate conserved amino acids. Triangles (red) indicate the position of the mutation in the *acc* allele.

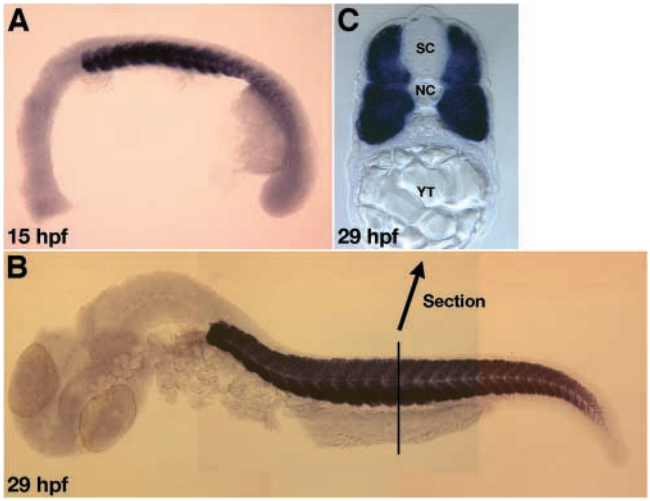

Fig. 6. SERCA1 mRNA is specifically expressed by muscles. Expression is observed only in muscles at 15 hpf (A) and 29 hpf (B). Axial section of 29 hpf embryos clearly shows exclusive expression in muscles (C). Expression is not observed in the spinal cord. SC, spinal cord; NC, notochord; YT, yolk tube.

point mutation in SERCA1 was found in all three alleles of *acc*. Ile97 in M2 was mutated to Asn in *acc*^{mi25i}; Ser766 in M5 to Phe in *acc*^{tq206}; and Thr848 in M7 to Ile in *acc*^{mi289a}. These missense mutations, which change the hydrophilicity/hydrophobicity properties of the amino acids, were found in transmembrane domains that were completely conserved among a variety of vertebrates (Fig. 5C). Previous structural and mutational analysis has suggested that these membrane domains turn or move during function and that most of the reported point mutations in these membrane domains disrupt or diminish the pump activity (reviewed by Toyoshima and Inesi, 2004; Wuytack et al., 2002). Thus, the *acc* mutations are likely to disrupt or reduce SERCA1 function.

As SERCA1 is found in the SR of muscle, *atp2a1* should be expressed in muscle. Indeed, in situ hybridization showed that *atp2a1* is expressed by axial muscles as early as 15 hpf, which precedes the appearance of motor behaviors (Fig. 6A,B). Cross-sections of the trunk showed that expression appears to be exclusively in muscles and not in the CNS (Fig. 6C). No expression of *atp2a1* in the CNS was observed at any level of the CNS (data not shown). Although expression of *atp2a1* in the CNS below the resolution of our in situ hybridizations cannot be excluded, muscle specific expression of *ATP2A1*is consistent with the primary *acc* defect found in muscles.

The molecular identification of *acc* as *atp2a1* encoding for SERCA1 was confirmed by mutant rescue and antisense phenocopy. We injected wild-type SERCA1 mRNA, SERCA1 mRNA carrying the *acc*^{tq206} mutation, or mRNA carrying a mutation at Pro789 to Leu [which is a cognate mutation reported in human Brody disease (see Discussion)] into recently fertilized embryos of *acc* heterozygous carriers. Nearly all the progeny injected with wild-type mRNA displayed normal coiling following touch at 24 hpf (Fig. 7B, 97.5%, 157/161), whereas only a few responded with the mutant phenotype (2.5%, 4/161). Approximately 25% of uninjected progeny (Fig. 7A, 28.6%, 16/56), *acc*^{tq206} mRNA-injected progeny (Fig. 7C, 23.2%, 29/125), and the Brody disease mRNA-injected progeny (Fig. 7D, 26.5%, 43/162) showed the mutant response, while the rest responded normally. As injection of mutant forms of the SERCA1 mRNA did not induce a higher incidence of embryos to respond aberrantly, they appear not to have a dominant effect. Because one would expect 25% of progeny to be mutant from a cross of heterozygous carriers, these results are consistent with rescue of normal touch responses by injection of wild-type mRNA. Furthermore, 35/157 (22.5%) of wild-type mRNA-injected embryos that responded normally at 24 hpf displayed the mutant response after 48 hpf, suggesting that the rescue by wild-type mRNA was transient (data not shown). This is probably due to degradation of the injected mRNA. As ~25% of the progeny recovered mutant responses, they were likely to be homozygous embryos that were rescued transiently by the wild-type mRNA.

To knockdown synthesis of SERCA1, antisense MO against SERCA1 mRNA was injected into recently fertilized wild-type embryos. Antisense MO-injected wild-type embryos displayed the *acc* behavior after touch (Fig. 7F, 92%, 33/36), whereas control MO-injected wild-type embryos did not (Fig. 7E, 0%, 0/17). The antisense MO was designed to block translation of endogenous SERCA1 mRNA but not the injected SERCA1 mRNA, owing to engineered differences in the 5′-untranslated sequence of the injected mRNA (see Materials and methods). When the antisense MO was co-injected with the engineered wild-type SERCA1 mRNA, the antisense MO phenotype was blocked and embryos responded normally to touch (Fig. 7G, 95%, 37/39). The inhibition of the SERCA1 knockdown

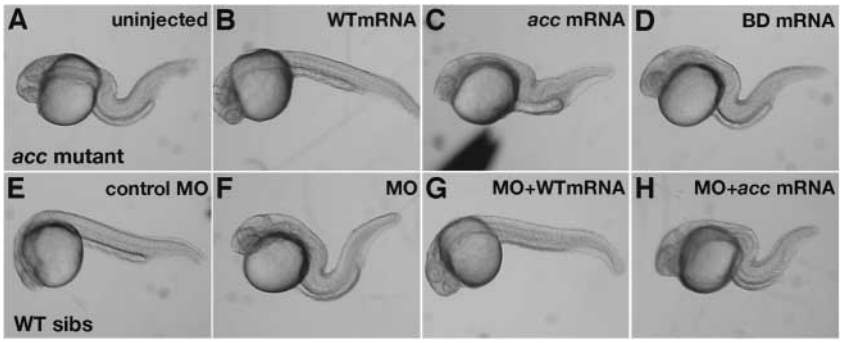

Fig. 7. Mutant rescue and antisense phenocopy confirm that *atp2a1* is the *acc* gene. All panels show video frames 1 second after touch. (A-D) Wild-type SERCA1 mRNA rescues the *acc* phenotype. Uninjected (A) and *acc*^{tq206} mRNA-injected (C) *acc* embryos respond with the aberrant dorsal bend following touch, while *acc* embryos injected with wild-type SERCA1 mRNA respond normally to touch (B). This embryo coiled twice and relaxed 1 second after touching. Injection of SERCA1 mRNA carrying a cognate Brody disease mutation does not rescue the *acc* phenotype (D). (E-H) Antisense *atp2a1*/SERCA1 phenocopies the *acc* phenotype. Antisense MO-injected wild-type embryos respond to touch with the dorsal bend (F), while control MO-injected embryos respond with coils and are relaxed 1 second after touching (E). Co-injection of wild-type SERCA1 mRNA with antisense MO blocks the induction of the mutant phenotype and shows the normal coils and relaxation to touch (G), whereas co-injection with mutant mRNA does not (H).

phenotype by wild-type mRNA was specific, as embryos injected with both antisense MO and *acc*^{tq206} mRNA showed *acc* behavior (Fig. 7H, 88%, *n*=28/32). Thus, wild-type SERCA1 mRNA rescue of *acc* mutants and antisense knockdown of SERCA1 confirm that *atp2a1*, encoding the SR Ca^{2+} pump SERCA1, is the responsible gene for *acc* mutation.

Discussion

acc mutants have a defect in muscle relaxation

Several findings demonstrate that *acc* embryos have a muscle relaxation defect. First, the kinetic analysis of the touch response and spontaneous coiling showed that the constant contraction and relaxation phases were significantly longer in *acc* embryos. Second, direct electrical stimulation of muscle demonstrated that *acc* muscles failed to follow stimulation at much lower frequencies compared with wild-type muscles. Third, in vivo imaging of Ca^{2+} transients revealed that the decay in cytosolic Ca^{2+} during relaxation was significantly slower in *acc* muscle. Fourth, the *acc* gene encodes for the muscle-specific SERCA1 Ca^{2+} pump. Therefore, slower reuptake of Ca^{2+} causes muscles to relax much more slowly. This results in slower spontaneous coiling and overlap of muscle contraction on the two sides of the trunk during touch-induced escape responses.

acc was originally proposed to have a neuronal defect because strychnine-treated embryos displayed *acc*-like bilateral muscle contractions (Granato et al., 1996). Although the primary defect in *acc* mutants is a muscle relaxation defect caused by mutations in muscle-specific SERCA1, it is possible that there might be a secondary neuronal defect that is due to deficient motility of mutants. So far, we have not detected a neuronal phenotype. We found that the voltage response of wild-type muscles to touch, when glycine-mediated inhibitory synaptic transmission is blocked by strychnine, is highly aberrant. By contrast, *acc* muscles exhibited normal rhythmic activity following mechanosensory stimulation. This along with the fact that the morphology of the nervous system is not obviously aberrant suggests that many features of the nervous system are normal. However, we cannot rule out a neuronal phenotype secondary to the primary muscle defect in *acc* embryos.

acc embryos also displayed morphological defects, such as a bent trunk, disrupted notochord and disturbed slow-twitch muscle fibers. These are secondary to the muscle relaxation defect, as paralysis by tricaine or N-benzyl-p-toluene sulphonamide prevented these morphological phenotypes. In fact, similar notochord and slow twitch defects are seen in another behavior mutant, *nic*$^{twister\ dbn12}$, that has a gain-of-function mutation in the α-subunit of the muscle-specific nicotinic acetylcholine receptor (Lefebvre et al., 2004). In *nic*$^{twister\ dbn12}$ homozygous mutant, prolonged neuromuscular transmission causes persistent activation of axial muscles bilaterally that results in *acc*-like hypercontractions and as a consequence cause notochord and slow twitch muscle abnormalities.

acc mutations are found in functionally important regions of SERCA1

We found three missense mutations that disrupt or diminish the SERCA1 function of *acc* mutants. Each mutation was located in a highly conserved α-helix, which forms a membrane domain. Most mutations introduced in M5 disrupt or severely reduce SERCA1 function in vitro, suggesting an essential role of the M5 domain (Sørensen, et al., 1997; Strock et al., 1998; Asahi et al., 1999; Guerini et al., 2000; Zhang et al., 2000; Ma et al., 2003; Dode et al., 2003). In fact, *acc*^{tq206} contains a mutation in the M5 domain that is consistent with the functional importance of the M5 for SERCA1 function. The structure and function of SERCA1 has been characterized by crystal structures in different states and by numerous point mutations. SERCA1 has two Ca^{2+}-binding sites: one consists of M5, M6 and M8; the other consists of M4 and M6 (Toyoshima et al., 2000). In M5, both Asn768 and Glu771 form hydrogen bond with Ca^{2+} by their side-chain oxygen atoms. During the conformational change from the Ca^{2+}-binding state to the dissociation state, the middle part of the M5 domain called the flexible hinge (Ile765-Asn768) tilts about 30°, whereas the adjacent lower region of M5 (Gly 770-Leu 777) hardly moves at all. This tilt results in turning the upper part of M5 and disrupts the hydrogen bond for Ca^{2+} binding (Toyoshima and Nomura, 2002; Nielsen et al., 2003). The mutation Ser766Phe found in *acc*^{tq206} is located in the hinge region and could account for the strongest phenotype.

During the conformational change of SERCA1, M4 inclines together with the M5 as a rigid body to induce movement of the M2 helix (Toyoshima and Nomura, 2002). This movement by M2 probably regulates the binding of sarcolipin, a regulator of SERCA1 in skeletal muscle (Odermatt et al., 1998; Asahi et al., 2002; MacLennan et al., 2003). Although this binding has not been studied structurally, a binding model between SERCA1 and phospholamban, a sarcolipin-like protein expressed in cardiac muscles (MacLennan and Kranias, 2003), suggests that the hydrophobic residues in the M2, including Ile97, are important for this interaction (Toyoshima et al., 2003; Asahi et al., 2003). The *acc*^{mi25i} allele has an Ile97Asn mutation in M2, suggesting that regulation of SERCA1 by sarcolipin may be aberrant in this allele. In contrast to the other membrane domains, M7 does not move much, because the M7 helix associates with the lower region of M5 (Toyoshima and Nomura, 2002), and M7 has not been well characterized by mutations. The fact that the *acc*^{mi289a} allele has a Thr848Ile mutation in M7 is the first functional evidence for a role of M7 for SERCA1 function.

acc mutants are an animal model for Brody disease

Brody disease is a rare inherited disorder of skeletal muscle function in humans. It is characterized by painless cramping induced by exercise and linked to an impairment of skeletal muscle relaxation (Brody, 1969). Most families harboring Brody disease show an autosomal recessive inheritance pattern and carry a mutation in the *ATP2A1* gene on chromosome 16 (Odermatt et al., 1996; Odermatt et al., 1997; Odermatt et al., 2000). In a minority of cases, Brody disease is inherited in an autosomal recessive pattern but there are no mutations in *ATP2A1* (MacLennan, 2000; Zhang et al., 1995) or in an autosomal dominant pattern with a (2;7) chromosomal translocation (Novelli et al., 2004). Thus, there are at least two genes other than *ATP2A1* that can give rise to Brody disease (MacLennan, 2000).

Among seven different SERCA1 mutations so far identified in Brody disease, five induce a stop codon 5′ to the Ca^{2+}-

binding sites and are considered to be null mutations (Odermatt et al., 1996; Odermatt et al., 1997; Odermatt et al., 2000). The other missense mutations are found in M6 and in a loop between the M6 and M7 (Odermatt et al., 2000). Surprisingly, the individuals that carry apparent null alleles of *ATP2A1* are able to relax their skeletal muscle albeit at a much slower rate without any obvious respiratory distress (MacLennan, 2000). Interestingly, SERCA1-null mice were defective in diaphragm function and died soon after birth, making them less attractive as an animal model for Brody disease (Pan et al., 2003). Compensatory or redundant mechanism for Ca^{2+} removal from the muscle cytosol in humans but not in mice, such as Na^{+}-Ca^{2+} exchangers, Ca^{2+}-ATPase in the plasma membrane, Ca^{2+} uptake by mitochondria and/or ectopic expression of other members of the SERCA family might account for the difference in viability between mouse and human (Wuytack et al., 2002).

In zebrafish, seven *acc* mutations were isolated in the Tübingen screen (Granato et al., 1996) and two in our ongoing screen. All of these mutations are autosomal recessive, suggesting the same inheritance as *ATP2A1* Brody disease. Zebrafish *acc* mutants and human Brody disease share the most crucial feature of aberrantly slow relaxation of muscles because of much slower reuptake of Ca^{2+} from the muscle cytosol to the SR caused by mutations in the *atp2a1* gene. Although zebrafish *acc* mutants die by day 10, their fast development and accessibility up to the time of death allows for detailed physiological analysis of the consequences of *atp2a1* mutations. As zebrafish embryos are readily accessible to molecular, genetic, pharmacological and physiological interventions, *acc* mutants could serve as an attractive animal model for Brody disease. For example, *acc* mutants could be used to screen for drugs that relieve the muscle defect in vivo by enhancing Ca^{2+} re-uptake or reducing Ca^{2+} release from the SR during a contraction. Interestingly, mutations in at least six genes in addition to *acc* can give rise to an *acc*-like behavioral phenotype in zebrafish (Granato et al., 1996). It would be interesting to see if any of these genes might also be genes that are associated with Brody disease.

We thank S. Sprague and L. Crowe for fish care, J. Manuel for generating F2 families, and R. Hume for helpful discussion and generous use of electrophysiology equipment. Supported by grants from the NINDS to J.Y.K. and Michigan Life Science Corridor to D.G. L.S.-A. was partly supported by a Fellowship from FRSQ. H.H. was supported by a Long Term Fellowship of the Human Frontier Science Program (HFSP).

Supplementary material

Supplementary material for this article is available at
http://dev.biologists.org/cgi/content/full/131/21/5457/DC1

References

Asahi, M., Kimura, Y., Kurzydlowski, K., Tada, M. and MacLennan, D. H. (1999). Transmembrane helix M6 in sarco(endo)plasmic reticulum Ca^{2+}-ATPase forms a functional interaction site with phospholamban. *J. Biol. Chem.* **274**, 32855-32862.

Asahi, M., Kurzydlowski, K., Tada, M. and MacLennan, D. H. (2002). Sarcolipin inhibits polymerization of phospholamban to induce superinhibition of sarco(endo)plasmic reticulum Ca^{2+}-ATPase (SERCAs). *J. Biol. Chem.* **277**, 26725-26728.

Asahi, M., Sugita, Y., Kurzydlowski, K., de Leon, S., Tada, M., Toyoshima, C. and MacLennan, D. H. (2003). Sarcolipin regulates sarco(endo)plasmic reticulum Ca^{2+}-ATPase (SERCA) by binding to transmembrane helices alone or in association with phospholamban. *Proc. Natl. Acad. Sci. USA* **100**, 5040-5045.

Bassett, D. I., Bryson-Richardson, R. J., Daggett, D. F., Gautier, P., Keenan, D. G. and Currie, P. D. (2003). Dystrophine is required for the formation of stable muscle attachments in the zebrafish embryo. *Development* **130**, 5851-5860.

Behra, M., Cousin, X., Bertrand, C., Vonesch, J. L., Biellmann, D., Chatonnet, A. and Strähle, U. (2002). Acetylcholinesterase is required for neuronal and muscular development in the zebrafish embryo. *Nat. Neurosci.* **5**, 111-118.

Benders, A. A. G. M., Veerkamp, J. H., Oosterhof, A., Jongen, P. J. H., Bindels, R. J. M., Smit, L. M. E., Busch, H. F. M. and Wevers, R. A. (1994). Ca^{2+} homeostasis in Brody's disease. *J. Clin. Invest.* **94**, 741-748.

Berchtold, M. W., Brinkmeier, H. and Müntener, M. (2000). Calcium ion in skeletal muscle: its crucial role for muscle function, plasticity, and disease. *Physiol. Rev.* **80**, 1215-1265.

Bernhardt, R. R., Chitnis, A. B., Lindamer, L. and Kuwada, J. Y. (1990). Identification of spinal neurons in the embryonic and larval zebrafish. *J. Comp. Neurol.* **302**, 603-616.

Brody, I. A. (1969). Muscle contracture induced by exercise. *New Eng. J. Med.* **281**, 187-192.

Buss, R. R. and Drapeau, P. (2000). Physiological properties of zebrafish embryonic red and white muscle fibers during early development. *J. Neurophysiol.* **84**, 1545-1557.

Buss, R. R. and Drapeau, P. (2001). Synaptic drive to motoneurons during fictive swimming in the developing zebrafish. *J. Neurophysiol.* **86**, 197-210.

Buss, R. R. and Drapeau, P. (2002). Activation of embryonic red and white muscle fibers during fictive swimming in the developing zebrafish. *J. Neurophysiol.* **87**, 1244-1251.

Cheung, A., Dantzig, J. A., Hollingworth, S., Baylor, S. M., Goldman, Y. E., Mitchison, T. J. and Straight, A. F. (2001). A small-molecule inhibitor of skeletal muscle myosin II. *Nat. Cell Biol.* **4**, 83-88.

Chitnis, A. B. and Kuwada, J. Y. (1990). Axonogenesis in the brain of zebrafish embryos. *J. Neurosci.* **10**, 1892-1905.

Cui, W. W., Saint-Amant, L. and Kuwada, J. Y. (2004). The *shocked* gene is required for the function of a premotor network in the zebrafish CNS. *J. Neurophysiol.* (in press).

Devoto, S. H., Melancon, E., Eisen, J. S. and Westerfield, M. (1996). Identification of separate slow and fast muscle precursor cells in vivo, prior to somite formation. *Development* **122**, 3371-3380.

Dode, L., Andersen, J. P., Leslie, N., Dhitavat, J., Vilsen, B. and Hovnanian, A. (2003). Dissection of the functional differences between sarco(endo)plasmic reticulum Ca^{2+}-ATPase (SERCA) 1 and 2 isoforms and characterization of Darier disease (SERCA2) mutants by steady-state and transient kinetic analyses. *J. Biol. Chem.* **278**, 47877-47889.

Downes, G. B. and Granato, M. (2004). Acetylcholinesterase function is dispensable for sensory neurite growth but is critical for neuromuscular synapse stability. *Dev. Biol.* **270**, 232-245.

Drapeau, P., Saint-Amant, L., Buss, R. R., Chong, M., McDearmid, J. R. and Brustein, E. (2002). Development of the locomotor network in zebrafish. *Prog. Neurobiol.* **68**, 85-111.

Eaton, R. C. and Farley, R. D. (1973). Development of the mauthner neurons in embryos and larvae of the zebrafish, *Brachydanio rerio*. *Copeia* **4**, 673-682.

Felsenfeld, A. L., Walker, C., Westerfield, M., Kimmel, C. and Streisinger, G. (1990). Mutations affecting skeletal muscle myofibril structure in the zebrafish. *Development* **108**, 443-459.

Fetcho, J. R. (1990). Morphological variability, segmental relationships, and functional role of a class of commissural interneurons in the spinal cord of goldfish. *J. Comp. Neurol.* **299**, 283-298.

Fetcho, J. R. (1992). The spinal motor system in early vertebrates and some of its evolutionary changes. *Brain Behav. Evol.* **40**, 82-97.

Fetcho, J. R. and O'Malley, D. M. (1997). Imaging neuronal networks in behaving animals. *Curr. Opin. Neurobiol.* **7**, 832-838.

Fill, M. and Copello, J. A. (2002). Ryanodine receptor calcium release channels. *Physiol. Rev.* **82**, 893-922.

Gates, M. A., Kim, L., Egan, E. S., Cardozo, T., Sirotkin, H. I., Dougan, S. T., Lashkari, D., Abagyan, R., Schier, A. F. and Talbot, W. S. (1999). A genetic linkage map for zebrafish: comparative analysis and localization of genes and expressed sequences. *Genome Res.* **9**, 334-347.

Gordon, A. M., Homsher, E. and Regnier, M. (2000). Regulation of contraction in striated muscle. *Physiol. Rev.* **80**, 853-924.

Granato, M., van Eeden, F. J. M., Schach, U., Trowe, T., Brand, M., Furutani-Seiki, M., Haffter, P., Hammerschmidt, M., Heisenberg, C. P., Jiang, Y. J. et al. (1996). Genes controlling and mediating locomotion behavior of the zebrafish embryo and larva. *Development* **123**, 399-413.

Grillner, S. (2003). The motor infrastructure: from ion channels to neuronal networks. *Nat. Rev. Neurosci.* **4**, 573-586.

Guerini, D., Zecca-Mazza, A. and Carafoli, E. (2000). Single amino acid mutations in transmembrane domain 5 confer to the plasma membrane Ca^{2+} pump properties typical of the Ca^{2+} pump of endo(sarco)plasmic reticulum. *J. Biol. Chem.* **275**, 31361-31368.

Hukriede, N. A., Joly, L., Tsang, M., Miles, J., Tellis, P., Epstein, J. A., Barbazuk, W. B., Li, F. N., Paw, B., Postlethwait, J. H. et al. (1999). Radiation hybrid mapping of the zebrafish genome. *Proc. Natl. Acad. Sci. USA* **96**, 9745-9750.

Korzh, V., Edlund, T. and Thor, S. (1993). Zebrafish primary neurons initiate expression of the LIM homeodomain protein Isl-1 at the end of gastrulation. *Development* **118**, 417-425.

Kudo, N., Nishimaru, H. and Nakayama, K. (2004). Developmental changes in rhythmic spinal neuronal activity in the rat fetus. *Prog. Brain Res.* **143**, 49-55.

Lefebvre, J. L., Ono, F., Puglielli, C., Seidner, G., Franzini-Armstrong, C., Brehm, P. and Granato, M. (2004). Increased neuromuscular activity causes axonal defects and muscular degeneration. *Development* **131**, 2605-2618.

Lewis, K. E. and Eisen J. S. (2003). From cells to circuits: development of the zebrafish spinal cord. *Prog. Neurobiol.* **69**, 419-449.

Li, W., Ono, F. and Brehm, P. (2003). Optical measurements of presynaptic release in mutant zebrafish lacking postsynaptic receptors. *J. Neurosci.* **19**, 10467-10474.

Li, Q., Shirabe, K. and Kuwada, J. Y. (2004). Chemokine signaling regulates sensory cell migration in zebrafish. *Dev. Biol.* **269**, 123-136.

Lorent, K., Liu, K. S., Fetcho, J. R. and Granato, M. (2001). The zebrafish *space cadet* gene controls axonal pathfinding of neurons that modulate fast turning movements. *Development* **128**, 2131-2142.

Ma, H., Inesi, G. and Toyoshima, C. (2003). Substrate-induced conformational fit and headpiece closure in the Ca^{2+} ATPase (SERCA). *J. Biol. Chem.* **278**, 28938-28943.

MacLennan, D. H. (2000). Ca^{2+} signaling and muscle disease. *Eur. J. Biochem.* **267**, 5291-5297.

MacLennan, D. H. and Kranias, E. G. (2003). Phospholamban: a crucial regulator of cardiac contractility. *Nat. Rev. Mol. Cell Biol.* **4**, 566-577.

MacLennan, D. H., Rice, W. J. and Green, N. M. (1997). The mechanism of Ca^{2+} transport by sarco(endo)plasmic reticulum Ca^{2+}-ATPase. *J. Biol. Chem.* **272**, 28815-28818.

MacLennan, D. H., Asahi, M. and Tupling, A. R. (2003). The regulation of SERCA-type pumps by phospholamban and sarcolipin. *Ann. N.Y. Acad. Sci.* **986**, 472-480.

Mullins, M. C., Hammerschmidt, M., Haffter, P. and Nüsslein-Volhard, C. (1994). Large-scale mutagenesis in the zebrafish: in search of genes controlling development in a vertebrate. *Curr. Biol.* **4**, 189-202.

Nielsen, G., Malmendal, A., Meissner, A., Møller, J. V. and Nielsen, N. C. (2003). NMR studies of the fifth transmembrane segment of sarcoplasmic reticulum Ca^{2+}-ATPase reveals a hinge close to the Ca^{2+}-ligating residues. *FEBS Lett.* **544**, 50-56.

Nüsslein-Volhard, C. and Dahm, R. (2002). *Zebrafish.* New York, NY: Oxford University Press.

Novelli, A., Valente, E. M., Bernardini, L., Ceccarini, C., Sinibaldi, L., Caputo, V., Cavalli, P. and Dallapiccola, B. (2004). Autosomal dominant Brody disease cosegregates with a chromosomal (2;7)(p11.2;p12.1) translocation in an Italian family. *Eur. J. Hum. Genet.* **12**, 579-583.

Odermatt, A., Taschner, P. E. M., Khanna, V. K., Busch, H. F. M., Karpati, G., Jablecki, C. K., Breuning, M. H. and MacLennan, D. H. (1996). Mutations in the gene-encoding SERCA1, the fast-twitch skeletal muscle sarcoplasmic reticulum Ca^{2+} ATPase, are associated with Brody disease. *Nat. Genet.* **14**, 191-194.

Odermatt, A., Taschner, P. E. M., Scherer, S. W., Beatty, B., Khanna, V. K., Cornblath, D. R., Chaudhry, V., Yee, W. C., Schrank, B., Karpati, G. et al. (1997). Characterization of the gene encoding human sarcolipin (SLN), a proteolipid associated with SERCA1: absence of structural mutations in five patients with Brody disease. *Genomics* **45**, 541-553.

Odermatt, A., Becker, S., Khanna, V. K., Kurzydlowski, K., Leisner, E., Pette, D. and MacLennan, D. H. (1998). Sarcolipin regulates the activity of SERCA1, the fast-twitch skeletal muscle sarcoplasmic reticulum Ca^{2+}-ATPase. *J. Biol. Chem.* **273**, 12360-12369.

Odermatt, A., Barton, K., Khanna, V. K., Mathieu, J., Escolar, D., Kuntzer, T., Karpati, G. and MacLennan, D. H. (2000). The mutation of Pro^{789} to Leu reduces the activity of the fast-twitch skeletal muscle sarco(endo)plasmic reticulum Ca^{2+} ATPase (SERCA1) and is associated with Brody disease. *Hum. Genet.* **106**, 482-491.

Ono, F., Higashijima, S. I., Shcherbatko, A., Fetcho, J. R. and Brehm, P. (2001). Paralytic zebrafish lacking acetylcholine receptors fail to localize rapsyn clusters to the synapse. *J. Neurosci.* **21**, 5439-5448.

Ono, F., Shcherbatko, A., Higashijima, S. I., Mandel, G. and Brehm, P. (2002). The zebrafish motility mutant *twitch once* reveals new roles for rapsyn in synaptic function. *J. Neurosci.* **22**, 6491-6498.

Ono, F., Mandel, G. and Brehm, P. (2004). Acetylcholine receptors direct rapsyn clusters to the neuromuscular synapse in zebrafish. *J. Neurosci.* **24**, 5475-5481.

Pan, Y., Zvaritch, E., Tupling, A. R., Rice, W. J., de Leon, S., Rudnicki, M., McKerlie, C., Banwell, B. L. and MacLennan, D. H. (2003). Targeted disruption of the *ATP2A1* gene encoding the sarco(endo)plasmic reticulum Ca^{2+} ATPase isoform 1 (SERCA1) impairs diaphragm function and is lethal in neonatal mice. *J. Biol. Chem.* **278**, 13367-13375.

Ribera, A. B. and Nüsslein-Volhard, C. (1998). Zebrafish touch-insensitive mutants reveal an essential role for the developmental regulation of sodium current. *J. Neurosci.* **15**, 9181-9191.

Roberts, A. (2000). Early functional organization of spinal neurons in developing lower vertebrates. *Brain Res. Bull.* **53**, 585-593.

Saint-Amant, L. and Drapeau, P. (1998). Time course of the development of motor behaviors in the zebrafish embryo. *J. Neurobiol.* **37**, 622-632.

Sepich, D. S., Wegner, J., O'Shea, S. and Westerfield, M. (1998). An altered intron inhibits synthesis of the acetylcholine receptor α-subunit in the paralyzed zebrafish mutant *nic1*. *Genetics* **148**, 361-372.

Shimoda, N., Knapik, E. W., Ziniti, J., Sim, C., Yamada, E., Kaplan, S., Jackson, D., de Sauvage, F., Jacob, H. and Fishman, M. C. (1999). Zebrafish genetic map with 2000 microsatellite markers. *Genomics* **58**, 219-232.

Sørensen, T., Vilsen, B. and Andersen, J. P. (1997). Mutation $Lys^{758} \rightarrow$ Ile of the sarcoplasmic reticulum Ca^{2+}-ATPase enhances dephosphorylation of E_2P and inhibits the E_2 to E_1Ca_2 transition. *J. Biol. Chem.* **272**, 30244-30253.

Strock, C., Cavagna, M., Peiffer, W. E., Sumbilla, C., Lewis, D. and Inesi, G. (1998). Direct demonstration of Ca^{2+} binding defects in sarco-endoplasmic reticulum Ca^{2+} ATPase mutants overexpressed in COS-1 cells transfected with adenovirus vectors. *J. Biol. Chem.* **273**, 15104-15109.

Summerton, J. and Weller, D. (1997). Morpholino antisense oligomers: design, preparation, and properties. *Antisense Nucleic Acid Drug Dev.* **7**, 187-195.

Toyoshima, C. and Inesi, G. (2004). Structural basis of ion pumping by Ca^{2+}-ATPase of the sarcoplasmic reticulum. *Annu. Rev. Biochem.* **73**, 269-292.

Toyoshima, C. and Nomura, H. (2002). Structural changes in the calcium pump accompanying the dissociation of calcium. *Nature* **418**, 605-611.

Toyoshima, C., Nakasako, M., Nomura, H. and Ogawa, H. (2000). Crystal structure of the calcium pump of sarcoplasmic reticulum at 2.6 Å resolution. *Nature* **405**, 647-655.

Toyoshima, C., Asahi, M., Sugita, Y., Khanna, R., Tsuda, T. and McLennan, D. H. (2003). Modeling of the inhibitory interaction of phospholamban with the Ca^{2+} ATPase. *Proc. Natl. Acad. Sci. USA* **100**, 467-472.

Treiman, M., Caspersen, C. and Christensen, S. B. (1998). A tool coming of age: thapsigargin as an inhibitor of sarco-endoplasmic reticulum Ca^{2+}-ATPase. *TiPS* **19**, 131-135.

Westerfield, M. (1995). *The zebrafish book*. Eugene, OR: University of Oregon.

Westerfield, M., Liu, D. W., Kimmel, C. B. and Walker, C. (1990). Pathfinding and synapse formation in a zebrafish mutant lacking functional acetylcholine receptors. *Neuron* **4**, 867-874.

Wuytack, F., Raeymaekers, L. and Missiaen, L. (2002). Molecular physiology of the SERCA and SPCA pumps. *Cell Calcium* **32**, 279-305.

Xiao, T., Shoji, W., Zhou, W., Su, F. and Kuwada, J. Y. (2003). Transmembrane sema4E guides branchiomotor axons to their targets in zebrafish. *J. Neurosci.* **23**, 4190-4198.

Zeller, J. and Granato, M. (1999). The zebrafish *diwanka* gene controls an early step of motor growth cone migration. *Development* **126**, 3461-3472.

Zeller, J., Schneider, V., Malayaman, S., Higashijima, S. I., Okamoto, H.,

Gui, J., Lin, S. and Granato, M. (2002). Migration of zebrafish spinal motor nerves into the periphery requires multiple myotome-derived cues. *Dev. Biol.* **252**, 241-256.

Zhang, J. and Granato, M. (2000). The zebrafish *unplugged* gene controls motor axon pathway selection. *Development* **127**, 2099-2111.

Zhang, Y., Fujii, J., Phillips, M. S., Chen, H. S., Karpati, G., Yee, W. C., Schrank, B., Cornblath, D. R., Boylan, K. B. and MacLennan, D. H. (1995). Characterization of cDNA and genomic DNA encoding SERCA1, the Ca^{2+}-ATPase of human fast-twitch skeletal muscle sarcoplasmic reticulum, and its elimination as a candidate gene for Brody disease. *Genomics* **30**, 415-424.

Zhang, Z., Lewis, D., Strock, C., Inesi, G., Nakasako, M., Nomura, H. and Toyoshima, C. (2000). Detailed characterization of the cooperative mechanism of Ca^{2+} binding and catalytic activation in the Ca^{2+} transport (SERCA) ATPase. *Biochemistry* **39**, 8758-8767.

Zhang, J., Malayaman, S., Davis, C. and Granato, M. (2001). A dual role for the zebrafish *unplugged* gene in motor axon Pathfinding and pharyngeal development. *Dev. Biol.* **240**, 560-573.